

SUPPLEMENTARY INFORMATION

Lipid-Encapsulated Silica Nanobowls as an Efficient and Versatile DNA Delivery System

Madhura Som^a, Ratnesh Lal^{b,c} and Victor Ruiz-Velasco^{d*}

^a Department of Nanoengineering, University of California, San Diego, 9500 Gilman Drive, La Jolla, CA 92093, USA

^b Department of Bioengineering, University of California San Diego, 9500 Gilman Drive, La Jolla, CA 92093, USA

^c Mechanical & Aerospace Engineering, University of California San Diego, 9500 Gilman Drive, La Jolla, CA 92093, USA

^d Department of Anesthesiology and Perioperative Medicine, Penn State College of Medicine, Hershey, PA 17033

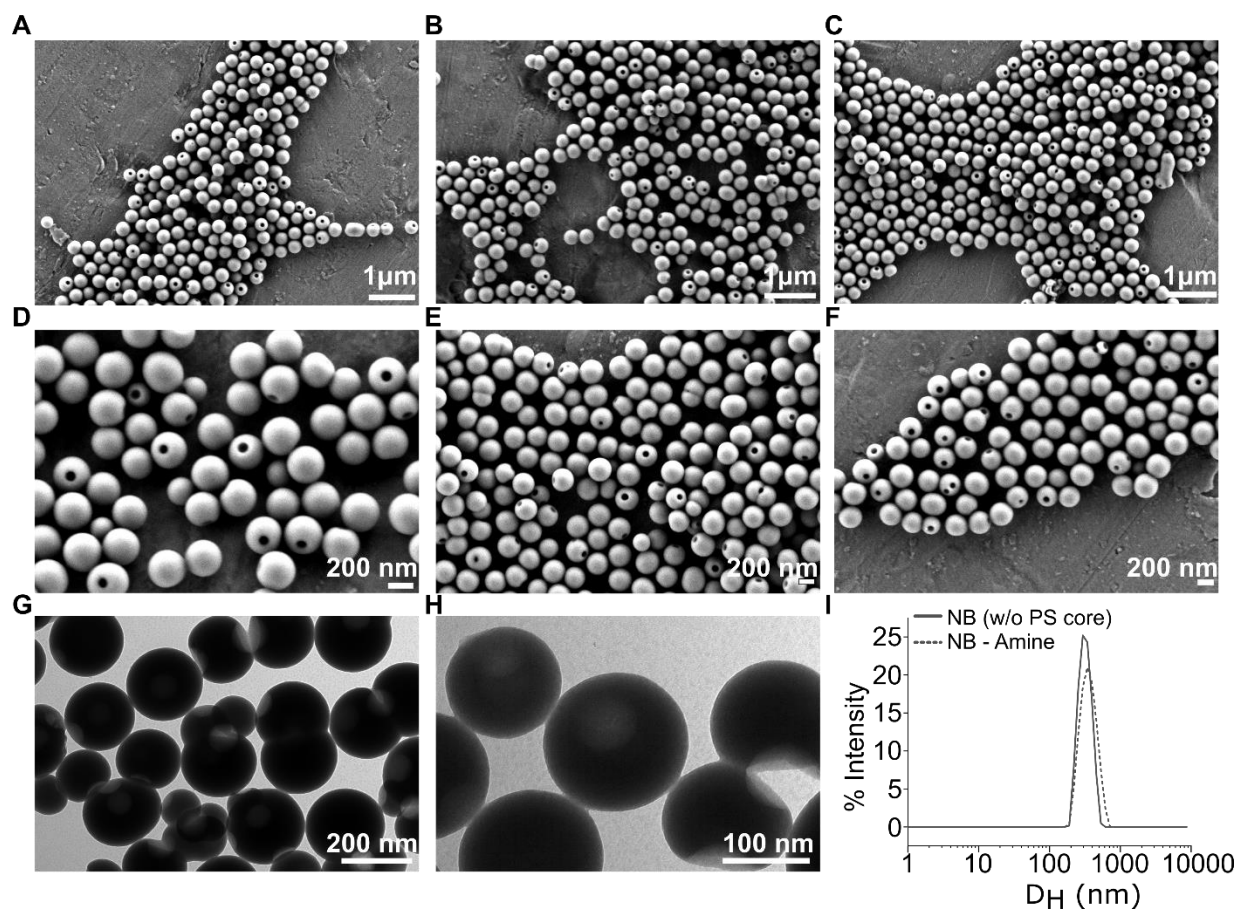


Figure S1. Characterization of NB size distribution. A-F. Scanning electron microscopy (SEM) and G-H. Transmission electron microscopy (TEM) images of DMF-washed, polystyrene core removed and purified silica NBs. I. Dynamic light scattering (DLS) raw intensity data showing a representative NB hydrodynamic size distribution in water before and after APTES (amine) functionalization.

| Sample | Hydrodynamic diameter (nm) | Polydispersity Index (PDI) | Zeta Potential (mV) |
|----------------------------------|----------------------------|----------------------------|---------------------|
| Nanobowls (no PS core) | 314.1 ± 6.6 | 0.032 ± 0.025 | -34.5 ± 0.6 |
| Nanobowls (Amine-functionalized) | 343.4 ± 5.3 | 0.114 ± 0.037 | $+36.8 \pm 0.8$ |

| | | | |
|---|------------------|-------------------|-----------------|
| NBs (Amine-functionalized, 10 $\mu\text{g}/\text{mg}$ plasmid loaded) | 370.1 ± 11.1 | 0.177 ± 0.033 | -49.0 ± 2.2 |
|---|------------------|-------------------|-----------------|

Table S1. Characterization of size and surface charge of NBs. The NBs were purified in each case as described in methods and re-dispersed at approx. 50 $\mu\text{g}/\text{ml}$ concentration in deionized water and measurements were acquired in triplicate. Error values reported are standard deviations for n=3 repeats.

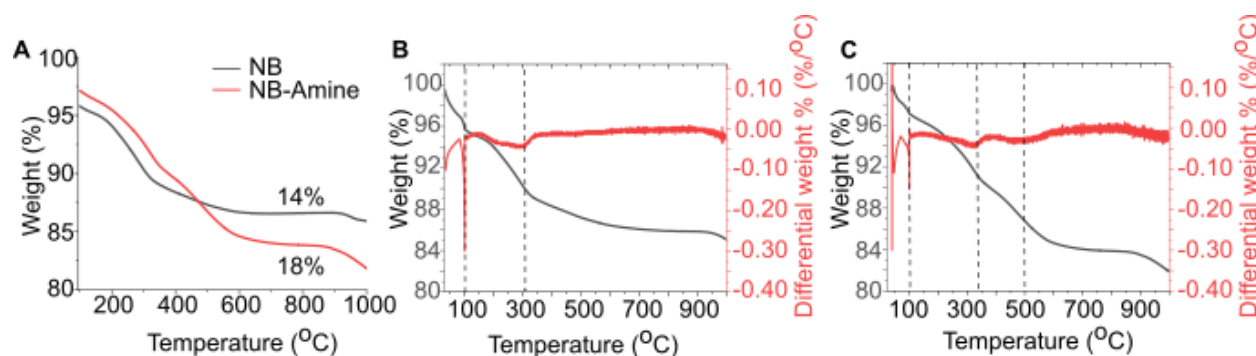


Figure S2. Thermogravimetric analysis (TGA) of NB and amine-functionalized NB. A. Total weight loss profile from 100-1000°C of NB (black) and amine-functionalized NBs (red). Individual weight loss (black) and differential of weight loss (red) are plotted with respect to temperature for B. NBs post-DMF wash and C. NBs coated with APTES post-DMF wash. Peaks (local minima) in the differential graphs indicate major regions of weight loss. Below 100°C, weight loss in both samples are caused by loss of adsorbed water. Between 100-300°C, weight loss is caused by loss of bound water and solvents like ethanol, DMF, etc. that are used in the synthesis and purification of NBs. These two mass losses are similar between both samples B and C. Above 300°C, the mass loss is higher in the amine functionalized NBs due to presence of bound amines from APTES salinization that burns off and causes weight loss between 300°C to 1000°C. Weight loss values in different temperature regimes are presented in Table S2.

| Temperature ranges | Materials contributing to weight loss | NB (% Weight loss) | | NB-Amine (% Weight Loss) | |
|----------------------------------|---------------------------------------|--------------------|----------|--------------------------|----------|
| | | Average | Std. Dev | Average | Std. Dev |
| Weight loss % \leq 100°C | Water | 4.25 | 0.03 | 2.88 | 0.02 |
| Weight loss % >100°C and < 300°C | Solvents | 5.66 | 0.25 | 5.60 | 0.66 |
| Weight loss % > 300°C | Other bound organics | 5.00 | 0.21 | 9.64 | 0.64 |

Table S2. TGA weight losses categorized in NBs and amine-functionalized NBs. The weight loss beyond 300°C in amine-functionalized NBs was first background subtracted from NB only sample. $4.64\% \pm 0.67\%$ net weight loss was determined to attribute to APTES based surface functionalization of NBs. Average and standard deviations are from duplicate measurements ($n=2$). This mass loss was calculated to be equivalent to $209.6 \mu\text{mol g}^{-1}$ APTES ($M_w=221.4 \text{ g/mol}$) loading. Alternatively, by considering mass loss of NB-Amine in 300-500°C and 500-1000°C regimes separately, and background subtracting from DMF washed NBs only, $5.21 \pm 0.91\%$ total mass loss is calculated which results in $236.7 \mu\text{moles g}^{-1}$. Assuming 1 mole of amine groups come from decomposition of 1 mole of APTES, we report here $209.6\text{-}236.7 \mu\text{moles g}^{-1}$ amine loading on the NBs.

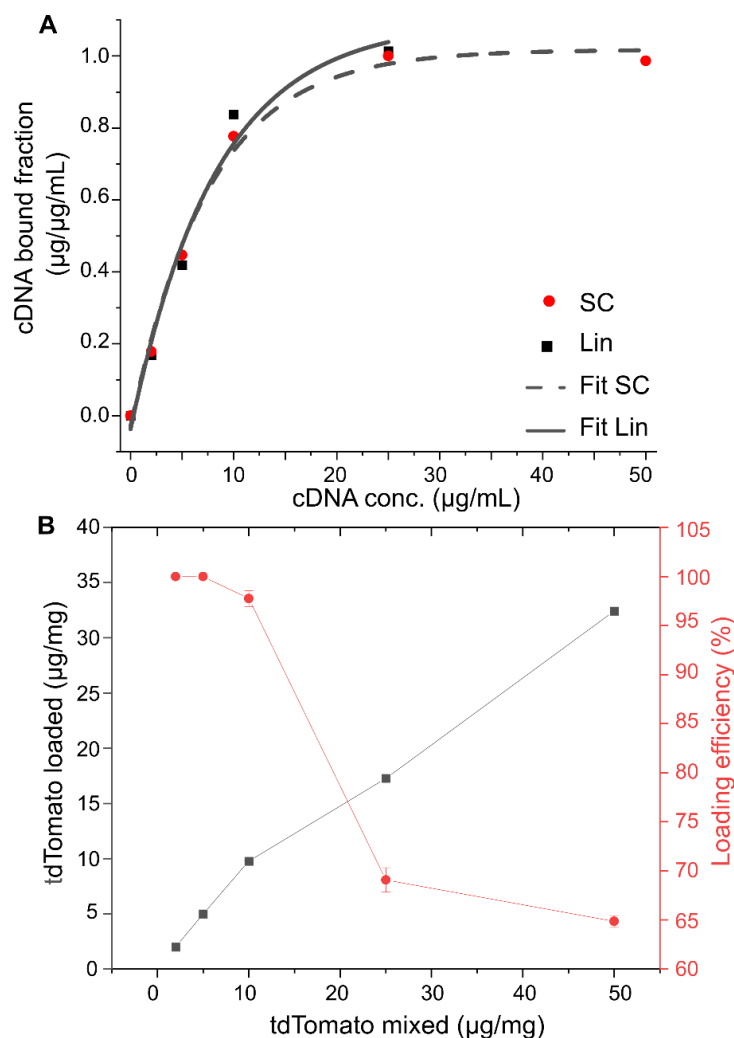


Figure S3. Analysis of linearized and supercoiled DNA loading on NB. A. Binding data for linear (Lin) and supercoiled (SC) clover were plotted and fitted. SC can be easily fit with an exponential increase model reaching a saturation plateau in the entire range from 0-50 $\mu\text{g}/\text{mg}$ DNA dosage (red circles and black dotted line). However, linearized DNA binding on NB does not follow the same pattern of saturating binding as supercoiled. We were able to fit linear loading data in the range $\leq 25 \mu\text{g}/\text{mg}$ (black squares and solid black line). In this range, the binding pattern follows an increasing exponential form, which is consistent between both types of DNA

constructs. Y-axis was normalized to saturation binding value of supercoiled at 50 $\mu\text{g/ml}$ and binding value of linearized at 25 $\mu\text{g/ml}$ within a scale of 0 to 1. B. Amount of tdTomato (linearized) cDNA loaded (black) and loading efficiency (red) at various amounts mixed with NBs (0-50 $\mu\text{g/mg}$). Red and black traces show representative loading profiles, with mean and $\pm\text{SEM}$ values, performed in duplicate.

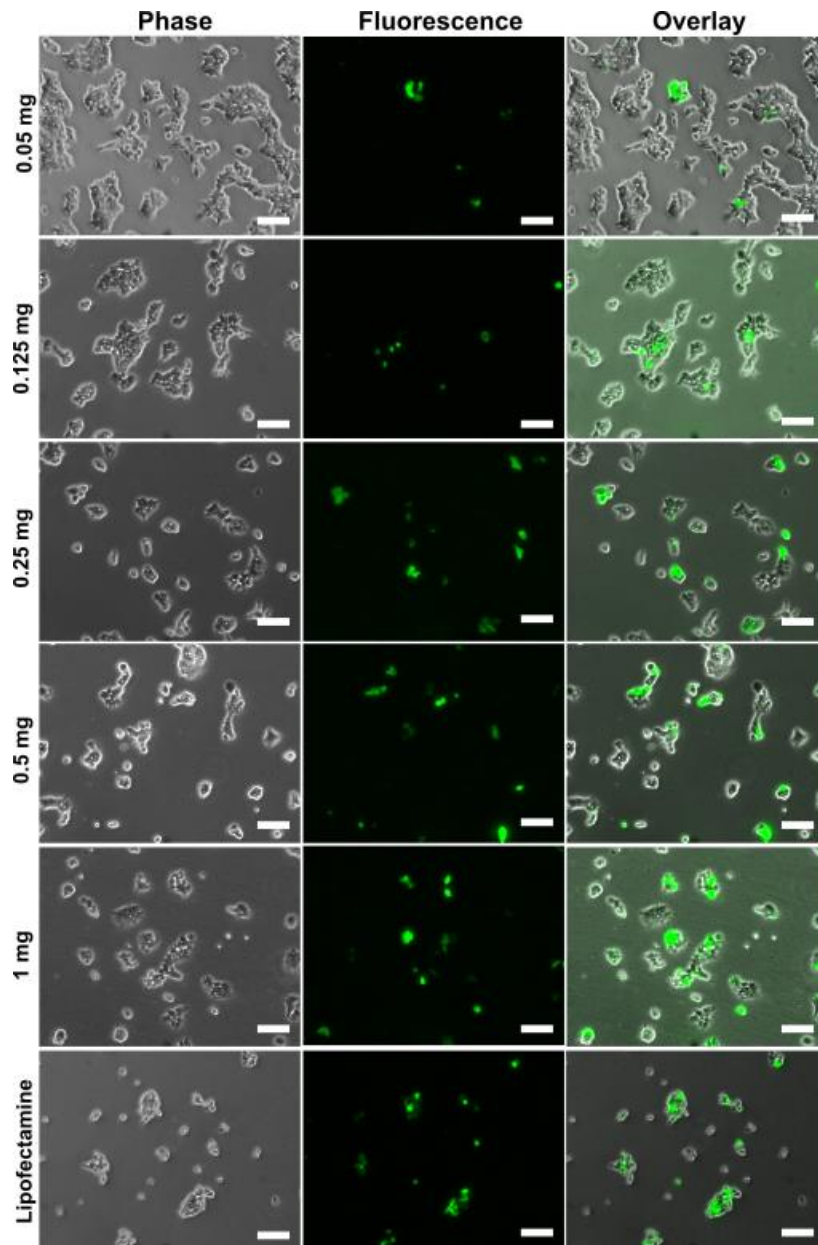


Figure S4. LNB dose-dependent transfection of HEK cells with linearized clover cDNA.

Phase (left), fluorescence (middle) and overlay (right) images acquired with a 10x objective of HEK cells 48 hrs post-transfection with varying concentrations of LNB (0.05-1 mg/ml) loaded with 10 µg/mg linearized clover cDNA. The samples were analyzed in flow cytometry for viability and toxicity trends (Figure 3E-F). Bottom row represents positive control used in flow cytometry with Lipofectamine 2000 (4 µg) 24 hrs post-transfection. All scale bars measure 100 µm.

| LNB conc. (mg/ml) | % Events from clusters | % Clover Positive, dead cells |
|---------------------------------------|-----------------------------------|--|
| 0.000 | 23 | N/A |
| 0.050 | 37 | 0.1 |
| 0.125 | 33 | 0.6 |
| 0.250 | 33 | 0.6 |
| 0.500 | 28 | 0.9 |
| 1.000 | 29 | 1.4 |

Table S3. LNB concentration dependent flow cytometry parameters. Cluster population % are reported above for all LNB concentrations tested with transfected HEK cells in flow cytometry assay. These events were gated out and were excluded from % GFP positive population analysis

(Figure 3F). Among the clover-expressing cells, further live/dead gating in the 7AAD channel (Quadrant II in Figure 3E) was applied to determine percentage of dead clover-expressing cells at various LNB transfection concentrations shown above.

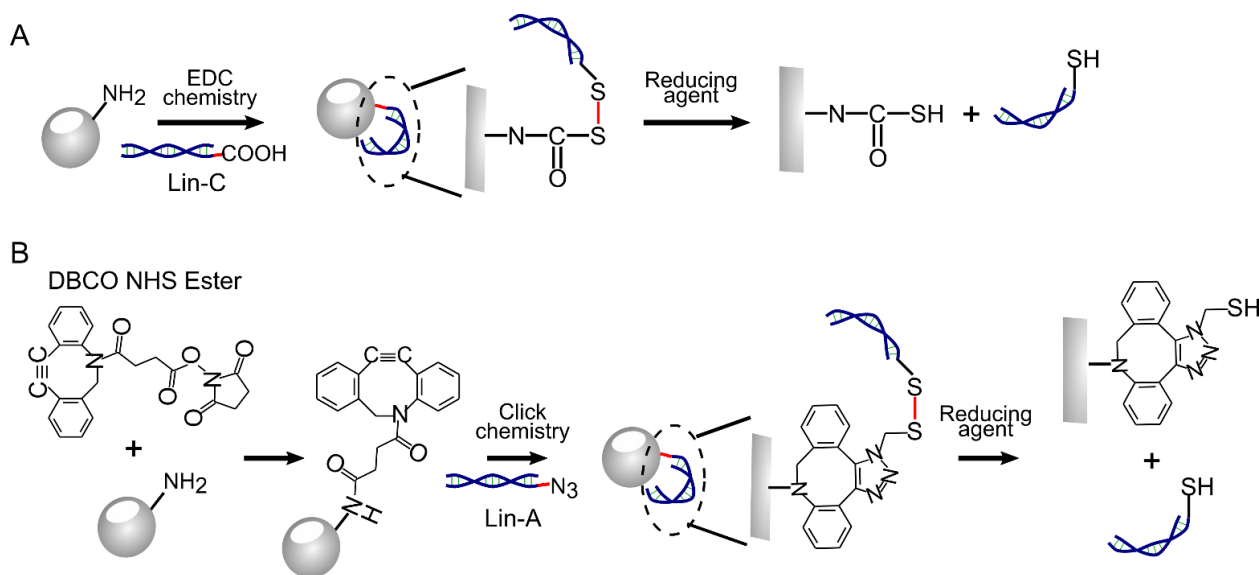


Figure S5. Types of linear DNA chemisorption schemes used with NBs A. Amine group on NB was covalently linked to carboxyl terminated linearized DNA with an EDC linker (EDC conjugation chemistry) B. Amine coated NBs were first conjugated with DBCO NHS ester to confer DBCO functionality on NBs followed by attachment of azido terminated linearized cDNA on DBCO functionalized NBs by click chemistry.

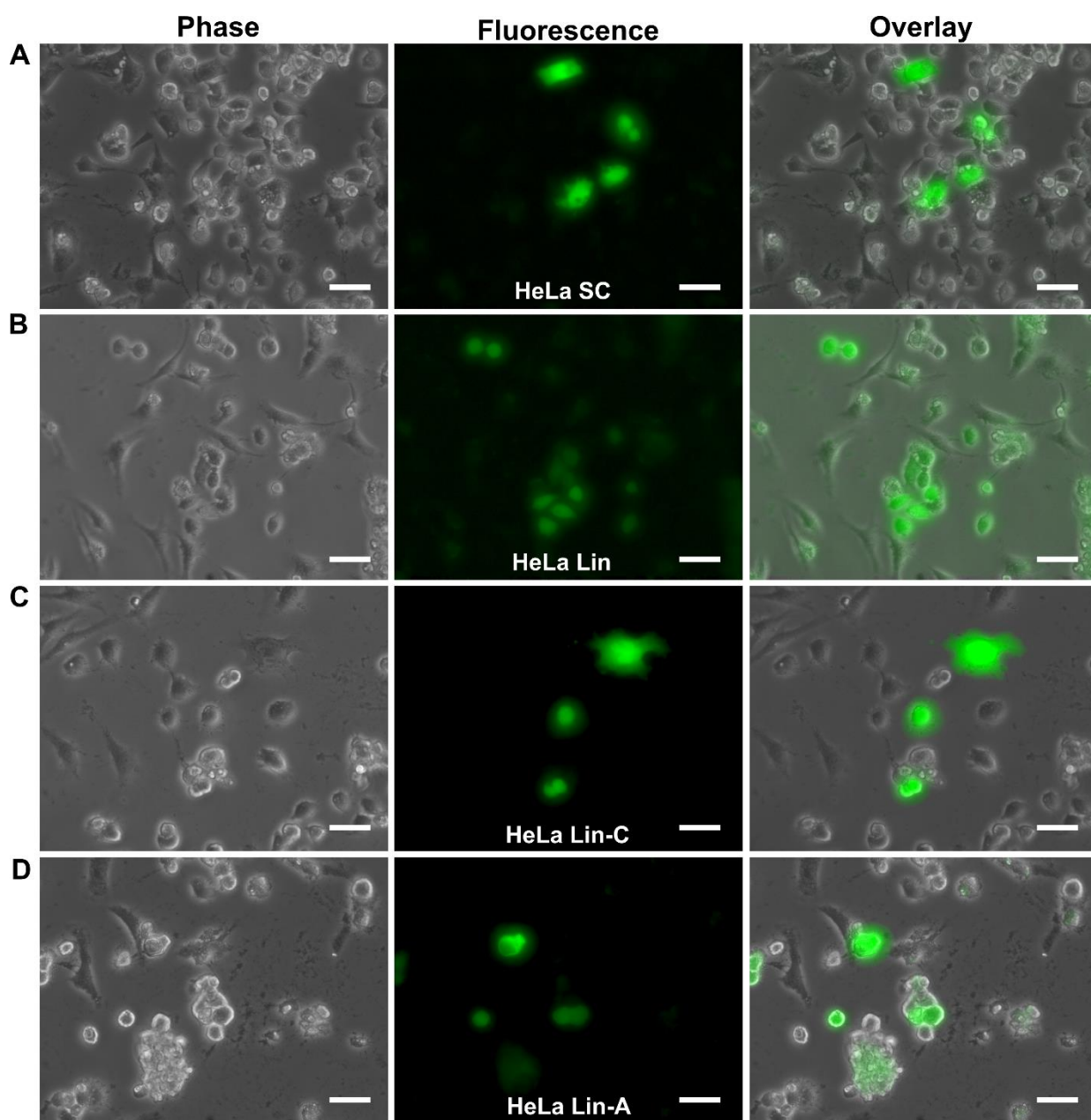


Figure S6. Transfection of HeLa cells with LNBs carrying 4 types of clover cDNA constructs.

HeLa cells were transfected for 4 hrs with 0.5 mg/ml LNB loaded with either supercoiled (SC) or linearized (Lin) or carboxylated linearized (Lin-C) or azido linearized (Lin-A) clover cDNA (10 μ g/mg). Phase (left), fluorescence images (middle) and overlay (right) were acquired with a 20x objective 48 hrs post-transfection. Scale bars indicate 50 μ m.

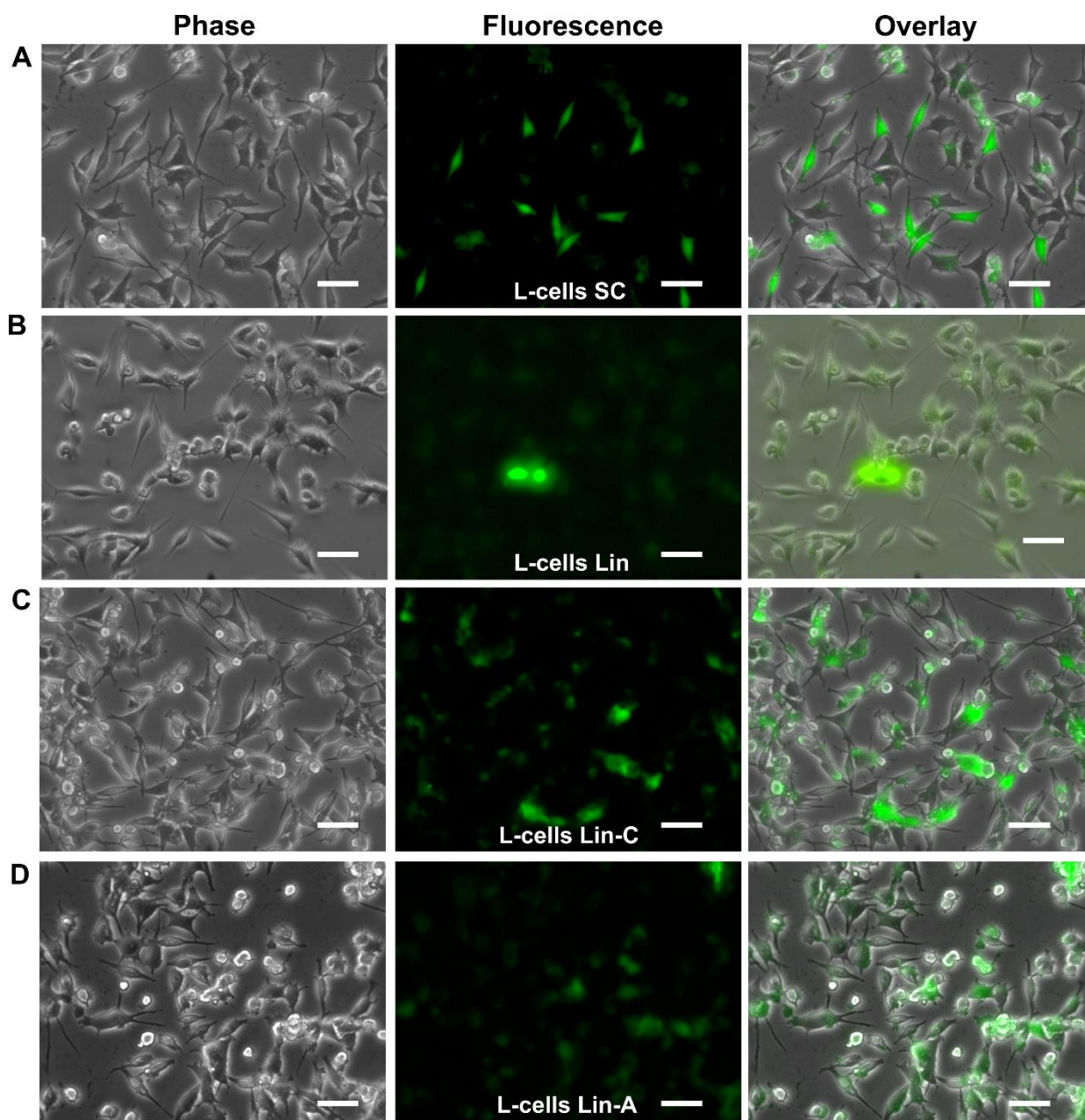


Figure S7. Transfection of L-cells with LNBs carrying 4 types of clover cDNA constructs. L-cells were transfected for 4 hrs with 0.5 mg/ml LNB loaded with either supercoiled (SC) or linearized (Lin) or carboxylated linearized (Lin-C) or azido linearized (Lin-A) clover cDNA (10 μ g/mg). Phase (left), fluorescence (middle) and overlay (right) images were acquired with a 20x objective 48 hrs post-transfection. Scale bars indicate 50 μ m.

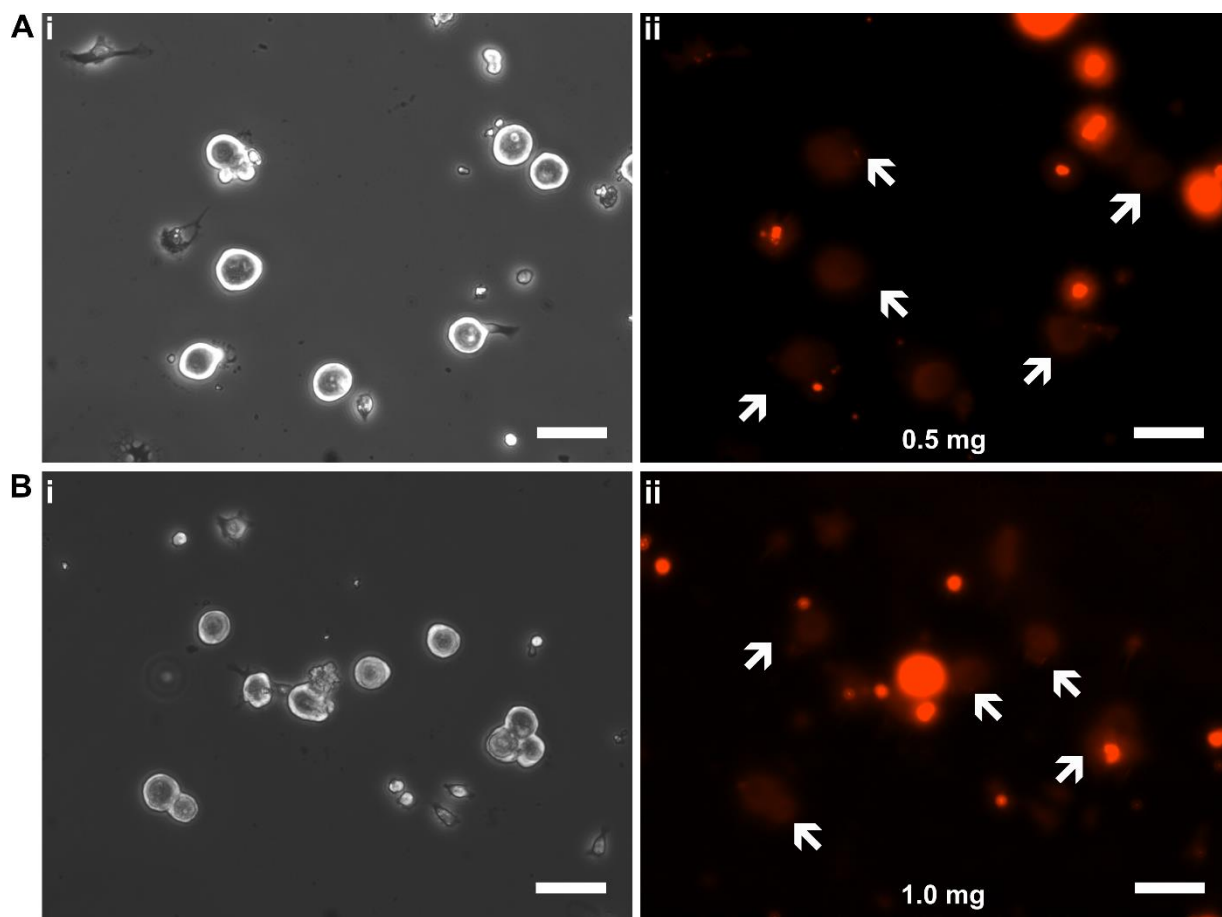


Figure S8. Internalization of Cy3-tagged LNPs in DRG tissue. A-B. Internalization of Cy3-tagged LNPs in rat DRG tissue incubated 6 hrs in (A) 0.5 or (B) 1 mg/ml Cy3-LNPs. The DRG tissue was enzymatically dissociated 6 hrs post-transfection period. Phase (i) and fluorescence images (ii) were acquired with a 20X objective. White arrows indicate dissociated neurons. Scale bars indicate 50 μ m.

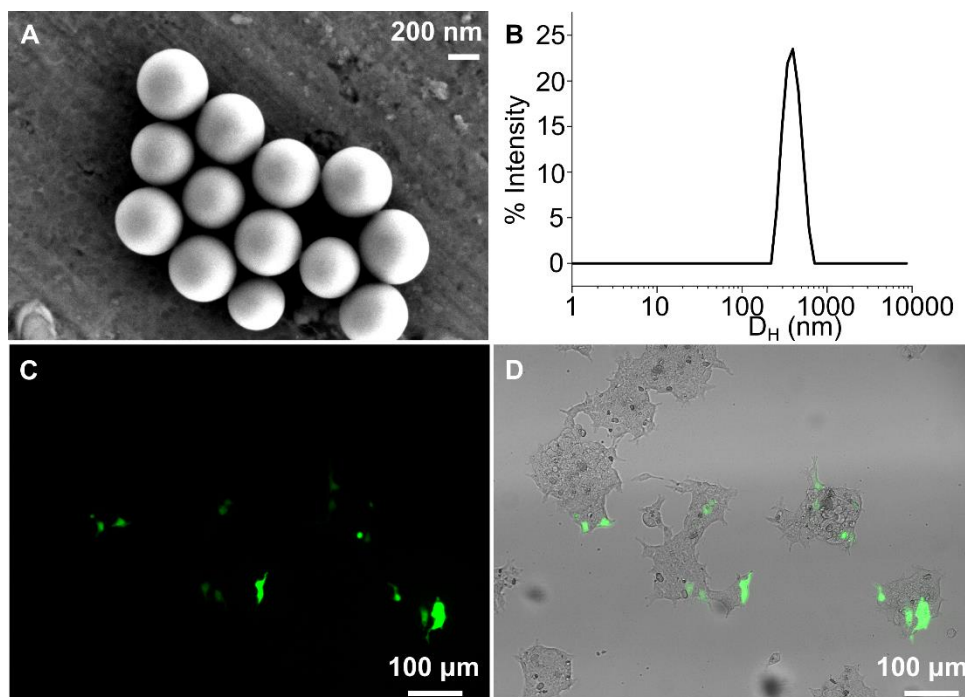


Figure S9. Transfection of HEK cells with DOPE/DOTAP encapsulated Stöber silica nanoparticles. A. Scanning electron microscopy (SEM) and B. Dynamic Light Scattering (DLS) characterization of Stöber silica nanoparticles after synthesis and purification. DLS data was acquired from $\sim 50 \mu\text{g/ml}$ silica nanoparticles dispersed in water. $D_H = 415.3 \pm 21.9 \text{ nm}$ $PDI = 0.207 \pm 0.043$ were measured. C-D Fluorescence microscopy images of 0.5 mg/ml clover cDNA loaded Stöber silica nanoparticles ($\sim 9 \mu\text{g}$ clover supercoiled plasmid per mg silica nanoparticles) 48 hrs post transfection in HEK 298 cells captured with a 10x objective. C. Fluorescence channel after pseudo coloring and D. Overlay of the fluorescence and the phase channels for the same field of view.